

Detection of white sand patches in central Amazonia using remote sensing and meteorological data

Nikolai S. Espinoza, Maria Teresa F. Piedade, Layon O. Demarchi, Gisiane R. Lima, Angélica F. Resende, Rosaria R. Ferreira, Francisco Alcinei G. Silva, Luiz Augusto T. Machado & Jochen Schörgart

To cite this article: Nikolai S. Espinoza, Maria Teresa F. Piedade, Layon O. Demarchi, Gisiane R. Lima, Angélica F. Resende, Rosaria R. Ferreira, Francisco Alcinei G. Silva, Luiz Augusto T. Machado & Jochen Schörgart (12 Mar 2025): Detection of white sand patches in central Amazonia using remote sensing and meteorological data, International Journal of Remote Sensing, DOI: [10.1080/01431161.2025.2476776](https://doi.org/10.1080/01431161.2025.2476776)

To link to this article: <https://doi.org/10.1080/01431161.2025.2476776>



Published online: 12 Mar 2025.



Submit your article to this journal [↗](#)



Article views: 120



View related articles [↗](#)



View Crossmark data [↗](#)



Detection of white sand patches in central Amazonia using remote sensing and meteorological data

Nikolai S. Espinoza^a, Maria Teresa F. Piedade^a, Layon O. Demarchi^a, Gisiane R. Lima^a, Angélica F. Resende^b, Rosaria R. Ferreira^b, Francisco Alcinei G. Silva^c, Luiz Augusto T. Machado^d and Jochen Schörgart^a

^aEcology, Monitoring and Sustainable Use of Wetlands (MAUA), National Institute for Amazonian Research (INPA), Manaus, Brazil; ^bDepartment of Forest Sciences, University of São Paulo (USP/ESALQ), Piracicaba, São Paulo, Brazil; ^cAmazon Tall Tower Observatory (ATTO), Large-Scale Biosphere-Atmosphere Experiment in the Amazon (LBA), National Institute for Amazonian Research (INPA), Manaus, Brazil; ^dDepartment of Applied Physics, University of São Paulo (USP), São Paulo, Brazil

ABSTRACT

Mapping the extent and different types of wetlands is essential in order to establish coherent policies for the sustainable management and protection of these important ecosystems. Few studies have been carried out on white-sand ecosystems (WSEs) in the Amazon based on the integration of meteorological data and remote sensing. In this study, the ability to identify the WSEs present in the Uatumã Sustainable Development Reserve (USDR) was evaluated using data on air temperature, land surface temperature (LST) and canopy height. Air temperature data was collected from a weather station at the USDR from January 2023 to September 2023. To indicate the WSEs areas present in the USDR, RGB images from Sentinel 2A and Planet/NICFI were used and to validate the areas of WSEs, high-resolution optical and thermal images were obtained using an unmanned aerial vehicle (UAV). In addition, satellite images from the TM and OLI/TIRS sensors on board the Landsat 5 and 8 satellites were used to obtain the LST variable. Additionally, canopy height data obtained by orbital lidar (NASA's Global Ecosystem Dynamics Investigation – GEDI) were applied. The meteorological station located in the open shrubby campinarana registered high temperatures during the analyzed period, with air temperatures over 30 °C in the afternoon, especially in the months with less rainfall. The LST and canopy height variables were efficient in mapping open shrubby habitats of the WSEs due to the fact that they present extremely high temperatures and relatively low canopies. Based on this method it was possible to calculate the WSEs coverage with a total area of 31.502 hectares, which is equivalent to around 7.4% of the USDR. The developed methodology in this study has huge potential to provide a reliable mapping and inventory of WSEs throughout the Amazon and the monitoring of the dynamics of these vulnerable ecosystems.

ARTICLE HISTORY

Received 16 September 2024
Accepted 3 March 2025

KEYWORDS

WSEs; central Amazonia; forest canopy height; land surface temperature

CONTACT Nikolai S. Espinoza ✉ nikosilvaespinoza@gmail.com Ecology, Monitoring and Sustainable Use of Wetlands (MAUA), National Institute for Amazonian Research (INPA), Avenida André Araújo 2936, Petrópolis, 69060001, Manaus, Amazonas, Brazil

1. Introduction

Wetlands (WLs) play an important role in maintaining hydrological and biogeochemical cycles, conserving biodiversity and safeguarding traditional and indigenous populations whose culture and livelihood are intrinsically related with these environments (Junk et al. 2014). Despite the diverse environmental services provided by WLs, these ecosystems have been drastically impacted in the Amazon by anthropogenic activities (Carvalho et al. 2021; Demarchi et al. 2024; Resende et al. 2019; Schöngart et al. 2021). The heterogeneity of climatic attributes, geological formation, varying flooding regime and types of water and soil, turn the Amazon basin into a hotspot of WL diversity with approximately 2.3×10^6 km² coverage (Fleischmann et al. 2022; Junk et al. 2011). These environments occur in the form of wetscapes or scattered in the matrix of non-flooded ecosystems.

To promote a sustainable development of these crucial environments, Brazilian WLs have been classified and inventoried based on the existing scientific knowledge WLs (Junk and Cunha 2024), providing information on ecology, distribution, management, threats and gaps of knowledge. The mapping and classification of WLs and their macrohabitats (smallest functional unit in the classification system with specific hydrological conditions and plant indicator species or groups) are of paramount importance to conserve these ecosystems and their biodiversity and promote sustainable use of their natural resources in the background of growing threats driven by climate and land-use changes (Maltchik et al. 2017).

For Amazon, the main types of WLs have been classified (Junk et al. 2011). In the case of the large Amazonian river-floodplains, the classification considers macrohabitats for the nutrient-poor black-water (igapó; Junk et al. 2012) and nutrient-rich whitewater floodplains (várzea; Junk et al. 2012), while other WL types still lack the classification. This holds for the white-sand ecosystems (WSEs), also known locally as ‘campinaranas’, which are oligotrophic plant formations occurring on sandy soils throughout the Amazon basin (Adeney et al. 2016; Anderson 1981; Demarchi et al. 2024). These ecosystems are characterized by having acidic soils with low fertility and are highly leached (Mendonça et al. 2015). Their vegetation ranges from grassy-woody habitats dominated by herbaceous plants, through shrubby areas with exposed soils, to arborized and forested physiognomies with marked stratification with canopy heights of 15–20 metres (Veloso, Rangel Filho, and Lima 1991; IBGE (2012); Demarchi et al. 2022).

During the dry season, the vegetation of the WSEs may go through periods with strong hydrological deficits due to the low water retention capacity of sandy soils (Franco and Dezzeo 1994). Furthermore, especially in more open habitats where there is exposed white sand and a high albedo, these ecosystems present high temperatures (Anderson 1981; Ribeiro and Santos 1975). Another important characteristic of many WSEs soils is the occurrence of a cemented layer (hardpan) a few metres deep, which causes the rise of the water table resulting in water logging or even shallow inundations (Damasco et al. 2013; Franco and Dezzeo 1994; Kubitzki 1989). These extreme environmental conditions set up strong filters selecting adapted species, which is reflected in the high percentage of plant endemism, estimated at 30% for tree and shrub vegetation in central Amazonia (Demarchi et al. 2022).

Although studies on WSEs have increased in recent years (Capurcho et al. 2020; Demarchi et al. 2024), these environments remain poorly studied in many parts of the

Amazonia, and there is little detailed information regarding their geographic distribution and physiognomic variation. The most recent estimates indicate a distribution of these ecosystems of approximately 335.000 km², which corresponds to 5% of the Amazonia, but this value is probably still underestimated (Adeney et al. 2016). WSEs form vast wetscapes spanning hundreds of square kilometres in northern Amazonia, encompassing a diverse range of macrohabitats (Fleischmann et al. 2022; Rosetti et al. 2019). However, in other regions of the Amazon, they appear as fragmented, island-like formations within the terra firme matrix, often covering just a few hectares (Prance 1996). These WSEs islands are very numerous in some regions in the Amazon and can often not be mapped and counted due to their small size (Adeney et al. 2016).

Research has demonstrated great advances in categorizing WLs through image segmentation and classification methods using machine-learning algorithms and SAR (Synthetic Aperture Radar) images (Belloli et al. 2022; Berhane et al. 2018; Dronova 2015; Fleischmann et al. 2022; Mahdianpari et al. 2019; Tian et al. 2016; X. Wang et al. 2019). Studies have been conducted in the Amazonia that applied remote sensing to evaluate vegetation patterns in floodplains (Ferreira-Ferreira et al. 2015; Resende et al. 2019) and terra-firme (de Almeida et al. 2025; Rennó et al. 2008) environments, and these have contributed to their characterization and the planning of strategies for the sustainable use of these ecosystems. However, for WSEs, very few studies have been carried out to refine their mapping and classification (Abraão et al. 2008; Adeney et al. 2016; Cordeiro and Rossetti 2015). The detection and accurate mapping of small WSE fragments, which are often overlooked in the Amazonian landscape remains a challenge. Considering the significant physiognomic and environmental variability of Amazonian WSEs and the growing threats affecting these ecosystems, the aim of this study is to develop a method by combining different remote sensors and integrating knowledge about this ecosystem to overcome the limitations of suitable methodologies for detecting and mapping small WSE patches (Adeney et al. 2016). The developed method allows further to differentiate physiognomies of these environments, which is of utmost importance to promote specific conservation strategies.

2. Material and methods

2.1. Study area

The study was performed in the Uatumã Sustainable Development Reserve (USDR), a state conservation unit (SCU) that is located at coordinates 59°10'/58°40'W and 2°27'/2°40'S, approximately 200 km northeast of the city of Manaus in the state of Amazonas (Figure 1 (a)). The USDR covers an area of 424.430 hectares (ha) and is located between the municipalities of Itapiranga and São Sebastião do Uatumã. Based on the Köppen-Geiger classification (Beck et al. 2018), the USDR has a humid tropical climate (A – Tropical Zone), with a prevailing tropical forest climate (Af). The average annual precipitation is over 2.000 mm·year⁻¹ and the average annual temperature around 27°C (Carneiro and Trancoso 2007). The precipitation cycle in the region presents its maximum values in March and April (~340 mm) and minimum values in August and September (~50 mm) (Andreae et al. 2015). The SCU is named for the Uatumã River, a black-water river draining the Guiana Shield (Piedade et al. 2025). The river presents a seasonal flow regime

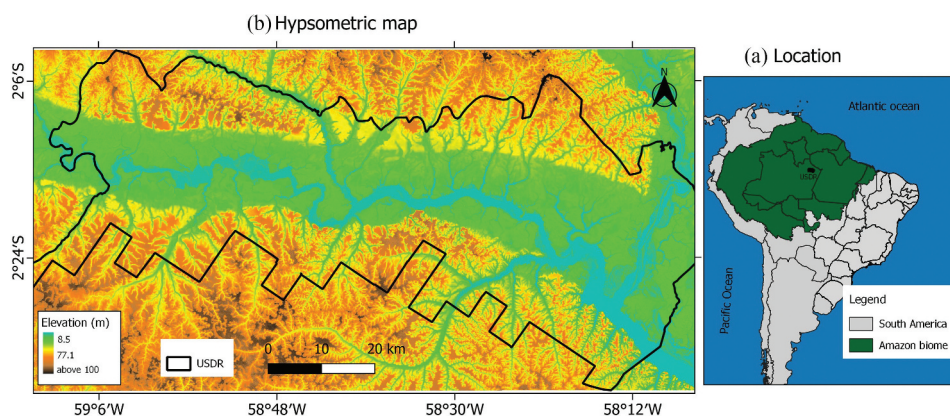


Figure 1. (a) Location of the study area and (b) Hypsometric map of the USDR from the copernicus DEM at a resolution of 30 m.

characterized by a monomodal flood pulse with one predictable high-water (May–July) and low-water period (October–November) with an annual amplitude of 6–9 m (Fassoni-Andrade et al. 2021). However, the flow regime in the western section of the USDR is impacted by the Balbina hydropower dam located 58 km upstream (linear distance), leading to massive disturbances in the floodplain forests of this region (Schöngart et al. 2021).

The landscape of the study region is quite heterogeneous, and the paedology and topography are relatively distinct (Figure 1(b)). At higher altitudes, dense and diverse ombrophilous forest phytophysionomies (terra-firme) with high canopies (>30 m height) occur on plateaus (>100 m above sea level – asl) and their slopes (>40 m asl), growing on deeply weathered nutrient-poor soils with a high clay fraction (latosols or ferralsols) (IDESAM (2009); Quesada et al. 2011, Andreae et al. 2015). Floodplains (igapós) occur at low altitudes (<30 m asl) along the drainage system formed by the Uatumã river and its major affluents (Resende et al. 2019). These environments are periodically inundated and the dominating vegetation form is forests with canopy heights below 30 metres, which are composed of distinct species when compared to those of the terra-firme and WSEs (Householder et al. 2024; Targhetta, Kesselmeier, and Wittmann 2015), growing on nutrient-poor, mainly clayish-silty soils (Lobo, Wittmann, and Piedade 2019). The intermediate elevations are characterized by ancient river terraces covered by dense and diverse ombrophilous forest with canopy heights over 30 metres growing on clayish soils and different physiognomies of WSEs on sandy soils with a vegetation cover of below 25 metres in height (Demarchi et al. 2022; Targhetta, Kesselmeier, and Wittmann 2015). Furthermore, wetlands on predominant sandy soils occur at these elevations in the form of palm swamps (*buritizal*) on almost permanently water-logged or shallowly flooded areas dominated by the species *Mauritia flexuosa* with heights <25 m and along low-order rivers riparian forests (*baixios*) with canopy heights >25 m height with frequent and unpredictable inundation patterns mainly during the rainy season.

This USDR is home to traditional populations of approximately 2.100 people living in 22 communities located on the banks of the Uatumã, Abacate and Jatapú rivers, whose subsistence is based on the sustainable use of natural resources adapted to local

ecological conditions (IDESAM 2010). In accordance with Brazilian environmental legislation, the USDR is divided into zones that guarantee the sustainable use of its natural resources, such as a strict protection zone for biodiversity and research (approximately 60% of the area), an extensive land use zone (approximately 35% of the area) and an intensive land use zone (approximately 5%). The zone of extensive use of timber and non-timber forest products covers all the areas along the Uatumã River and its main tributaries, as well as alluvial plains and adjacent paleofluvial terraces. Areas of intensive use for agriculture, livestock production and residences are located close to the communities (IDESAM 2009).

2.2. Dataset used

2.2.1. Meteorological data

The air temperature and precipitation data used in this study were obtained from a meteorological station of the Amazon Tall Tower Observatory project (ATTO-Campina site). The ATTO-Campina site is located within the USDR at the coordinates of $2^{\circ}10'S/59^{\circ}10'W$ and equipped with several atmospheric measurement instruments in a shrubby campinarana (Figure 2(a)). The meteorological station is installed on the surface, on a 2 metres high tripod and is equipped with sensors programmed to perform measurements of wind speed and direction, precipitation, temperature and relative air humidity, atmospheric pressure, and precipitation every minute (Figure 2(b)). A thermohygrometer (Delta Ohm) and a rain gauge (TB4, Hydrological Service) were used to quantify air temperature and precipitation from January 2023 to October 2023. The air temperature data were resized (resample) every minute to evaluate the hourly and daily variation of this variable in the shrubby campinarana environment.

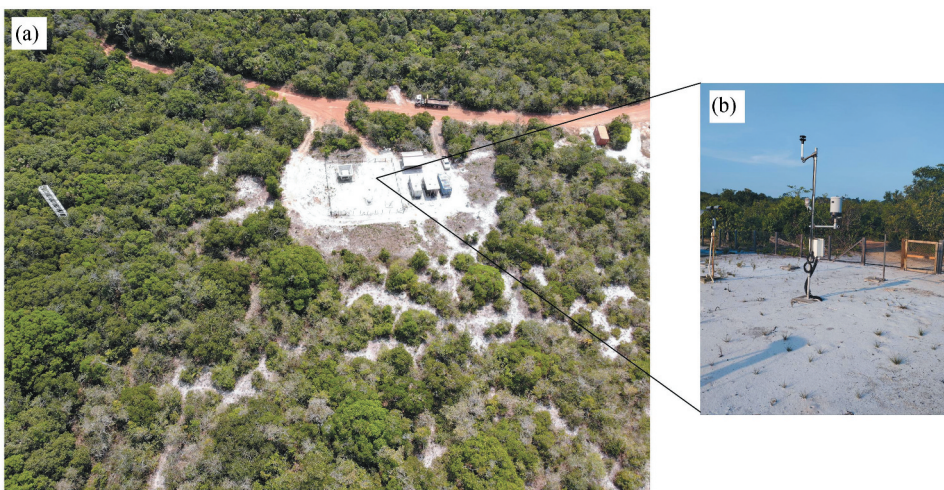


Figure 2. (a) Aerial image of the ATTO-Campina site and (b) Automatic weather station installed at the ATTO-Campina site.

2.2.2. Vegetation data

WSEs are observed throughout the USDR, and the species composition and vegetation structure are defined mainly depending on the variation in the water table and soil characteristics (Demarchi et al. 2022; Targhetta, Kesselmeier, and Wittmann 2015) grouped the existing habitats into three physiognomies, the shrubby campinarana that form islands of vegetation dominated by shrubs and small trees of up to 4 metres with patches of exposed sandy soils; arborized campinarana with a closed canopy of around 10 metres in height; and forested campinarana with clear stratification and a canopy measuring around 20 metres in height and the presence of some emergent trees. Furthermore, each of these habitats has a subdivision, with open habitats that have a deeper water table and low vegetation density or dense habitats that have a shallow water table and high vegetation density. A total of 167 species of trees and shrubs were recorded in the WSEs of the USDR, of which approximately 30% are considered endemic species (Demarchi et al. 2022). These oligotrophic plant formations in sandy soils are fragmented, distributed in patches of varying size and are interspersed between terra-firme and igapó environments.

2.2.3. Remote sensing data

To classify the WSEs in the USDR, a set of remote-sensing data from different sensors and platforms was used (Table 1).

2.2.3.1. Landsat data. Several Landsat 5 TM and Landsat 8 OLI/TIRS satellite images were used as one scene does not cover the total area of the USDR. Most of the images were chosen for the least rainy period in the region, with a minimum amount of cloud cover, thus contributing to a better visualization of the images and obtaining surface parameters (Table 2). In total, 18 images were selected for the 2 scenarios (Orbit: 230/Point:61; Orbit:230/Point:62), 14 from Landsat 5 TM (for the years 1985, 1987, 1995, 2008 and 2011) and four from Landsat 8 OLI/TIRS (2016 and 2020).

The spectral bands B3 (red) and B4 (near infrared) of Landsat 5 TM with a spatial resolution of 30 metres and thermal band B6 with a spatial resolution of 120 metres were used. For Landsat 8 OLI/TIRS, the spectral bands B4 (red) and B5 (near infrared) were used with a spatial resolution of 30 metres and the thermal band B10 with 100 metres of spatial resolution. The images were obtained from the website of the United States Geological

Table 1. Summary of the datasets used.

Data or image	Type	Category	Bands, sensors, or cameras	Spatial resolution (m)
Sentinel 2A	Raw data	Optical	RGB	10
Planet/NICFI	Product derived (mosaic)	Optical	RGB	4.8
Soil sand content	Product derived (mosaic)	-	-	90
UAV	Raw data	Optical and Infrared	RGB and Thermal	Very high resolution (VHR)
Landsat 5	Raw data	Optical and Infrared	Red and Near Infrared	30 and 120
Landsat 8	Raw data	Optical and Infrared	Red and Near Infrared	30 and 100
GEDI	Product derived (mosaic)	Optical and Lidar	-	30

Survey (USGS) (<http://earthexplorer.usgs.gov>). Using the bands of the Landsat 5 TM and Landsat 8 OLI/TIRS satellites, several processes were carried out in a GIS environment to measure land surface temperature (LST). To better understand the various stages of image processing, the methodology proposed by Ndossi and Avdan (2016) was used to obtain the surface temperature.

2.2.3.2. Sentinel 2A data. For the entire period of data from the Sentinel 2A satellite, two images were obtained with the lowest percentage of clouds, since only one image would not cover the total area of the USDR. Therefore, surface reflectance data was obtained for 31 July 2020 using the Google Earth Engine (GEE), and bands B2 (blue), B3 (green) and B4 (red) of the Multispectral Sensor Instrument (MSI) with a spatial resolution of 10 metres were selected, orthorectified and atmospherically corrected. Using Geographic Information Systems (GIS) techniques, the bands were composed and the images were mosaicked.

2.2.3.3. Unmanned aerial vehicle (UAV) data. To validate the areas of WSEs obtained from satellite images, flights were carried out with UAV (DJI, Mavic 2 Enterprise Dual) in the study area. This UAV features a fully stabilized 3-axis gimbal camera with an infrared thermal camera and a visual camera, simultaneously providing 12-megapixel visible light and infrared images. In the years 2022 and 2023, field expeditions were carried out at the USDR to identify and validate the open areas of campinaranas and obtain georeferenced images. In total, six open campinaranas complexes were mapped in the USDR using UAV images: three along the Uatumã river, two in the adjacent area of the ATTO-Campina site and one along the Abacate River (Figure 3).

2.2.3.4. Planet/NICFI data. The Norwegian International Climate and Forests Initiative (NICFI) provides high-resolution mosaics of Planet images for monitoring tropical forests, covering the area between 30° N and 30° S (<https://planet.com/nicfi/>). In this study, monthly 'Tropical Americas' mosaics were obtained from this platform for the period from June 2020 to December 2021 using bands B (blue), G (green) and R (red) with a spatial resolution of 4.8 metres. Using the GEE tool, the filter was applied to select only the USDR. The images were averaged to eliminate the months that had a large amount of cloud cover and the composition process of the bands and mosaic of the images was carried out.

2.2.3.5. Global forest canopy height (CH) data. The canopy height data used in this study were obtained by integrating forest structure measurements using Light Detection and Ranging (Lidar) GEDI and Landsat data time series with 30-metre spatial resolution (Potapov et al. 2021). NASA GEDI is a Lidar instrument aboard the International Space Station since April 2019. It provides measurements of vegetation structure, including forest canopy height between 52°N and 52°S. Data is aggregated into continental mosaics, with the height of the canopy represented in metres. The research proposed by Potapov et al. (2021) shows the methodology used to obtain forest canopy height data. The canopy height model saturates above 30 metres and does not adequately represent taller trees and is quite representative for the classification of WSEs given that these ecosystems have tree canopies of up

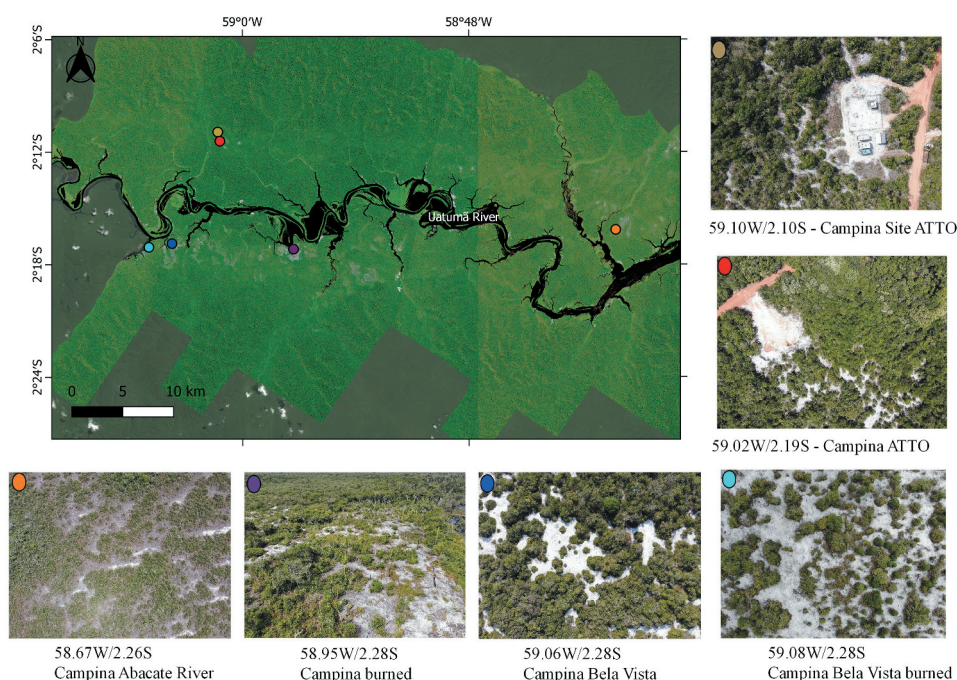


Figure 3. RGB composite from the sentinel-2A satellite at 10 m resolution in the USDR, along with high-resolution RGB images 12 MP from the UAV.

to 25 metres in the USDR (Demarchi et al. 2022). For this study, canopy height data from the South American continental mosaic was used, which can be accessed through the GEE or by downloading it directly from the website (<http://glad.umd.edu/dataset/gedi/>).

2.2.3.6. Brazilian soil sand content data. The soil sand content map used in this study was made available by Embrapa with a spatial resolution of 90 metres (Vasques et al. 2021). In this study, a layer of 100–200 cm of sand content in the soil was used to delimit the areas of WSEs in the USDR.

2.3. Classification of WSE in the USDR

The first stage consisted of detecting the areas of WSEs using high and medium-spatial-resolution optical sensors. To identify and validate areas of WSEs, images from Sentinel 2A, Planet/NICFI, soil sand content map of Brazil (available at the Brazilian Agricultural Research Corporation – Embrapa platform), and high-resolution UAV images were used. To classify the WSEs areas, satellite data from Landsat and GEDI were used.

Finally, the classification stage of the WSEs in the USDR was carried out based on surface temperature variables through the processing of Landsat 5 and 8 images and height data from the global forest canopy of the GEDI. First, the two scenes were mosaicked and cropped for the USDR area, and then the average surface temperature in the images was calculated to determine the classification of the WSEs. Subsequently, using Boolean

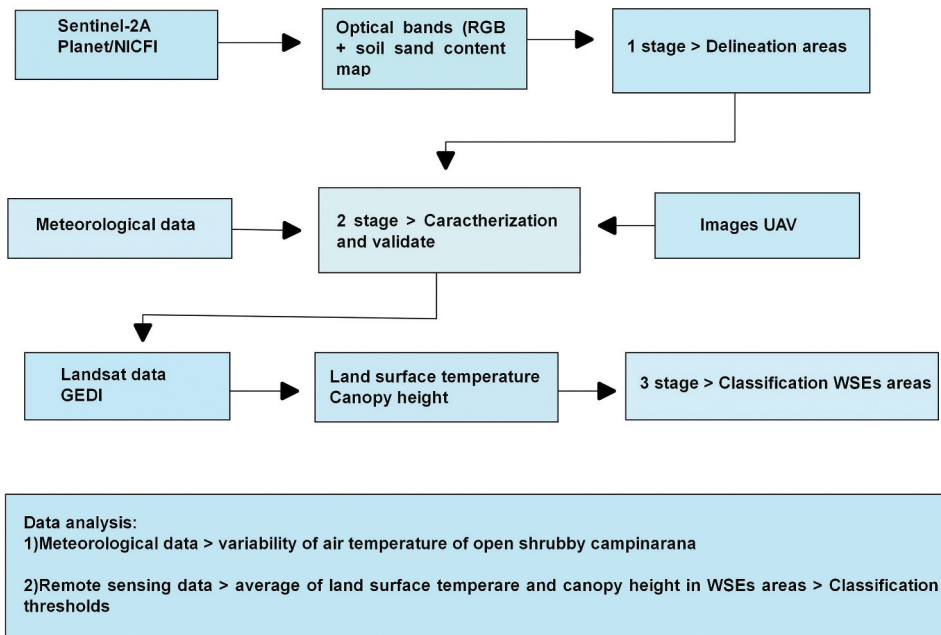


Figure 4. Methodological flowchart showing the sequential steps of classification WSEs areas in the USDR.

methods, it was possible to define the regions with WSEs through certain pixels by masking canopy height and average surface temperature values. Therefore, we grouped the habitats into two categories: shrubby (grouping shrubby and arborized campinaranas) with a canopy up to 10 metres and an average surface temperature of over 28°C, obtained from Equation (1), and forested areas with a canopy up to 25 metres and an average surface temperature between 26°C and 28°C, for which Equation (2) was used. While preparing the classification, refinement was applied through visual interpretation and manual vectorization using GIS tools to eliminate pixels that did not correspond to the areas of WSEs.

$$\text{Shrubby Campinaranas} = CH \leq 10 \text{ AND } LST > 28 \quad (1)$$

$$\text{Forest Campinaranas} = 10 < CH < 25 \text{ AND } 26 \leq LST < 28 \quad (2)$$

Where CH is the canopy height in metres, and LST corresponds to the average land surface temperature in °C.

The mapped and classified WSEs were overlapped with the shapefile of the ecological-economic zonation of the USDR (IDESAM 2010) to calculate the occurrence of shrubby and forested campinaranas in the three major zones. Figure 4 shows the main steps of the methodology applied in the study.

3. Results and discussion

3.1. Delineation of WSEs in the USDR

Satellite images from Sentinel 2A and Planet/NICFI helped to recognize patterns of WSEs in the USDR, mainly open shrubby campinaranas. It was observed that areas of open shrubby campinaranas with exposed sand obtained from the RGB composition of the Sentinel 2A and Planet/NICFI optical sensors (A, B, C, D, E and F) agreed with the occurrence of sandy soils (Figure 5). WSEs areas had a sand content of over $450 \text{ g}\cdot\text{kg}^{-1}$, while other vegetation types at higher altitudes and close to the Uatumā river had a lower sand concentration ($<300 \text{ g}\cdot\text{kg}^{-1}$). From the sand content map, it was possible to create a shape to indicate the potential occurrence of open shrubby campinaranas in the USDR.

3.2. Air and surface temperature in WSEs

In the open shrubby campinaranas, high temperatures have been observed due to the greater penetration of sunlight that falls on the partially exposed sandy soil, which heats up fast due to its lower specific heat (Alnefaie and Abu-Hamdeh 2020). These characteristics contributed to a warmer environment than forested areas on higher elevations without exposed soil. High temperatures of WSEs patched had already been recorded by Ribeiro and Santos (1975) at the Campina Reserve at INPA, 40 km north of Manaus (linear distance of about 100 km to USDR) with soil temperature of up to 42°C in the open shrubby vegetation with the presence of exposed sand.

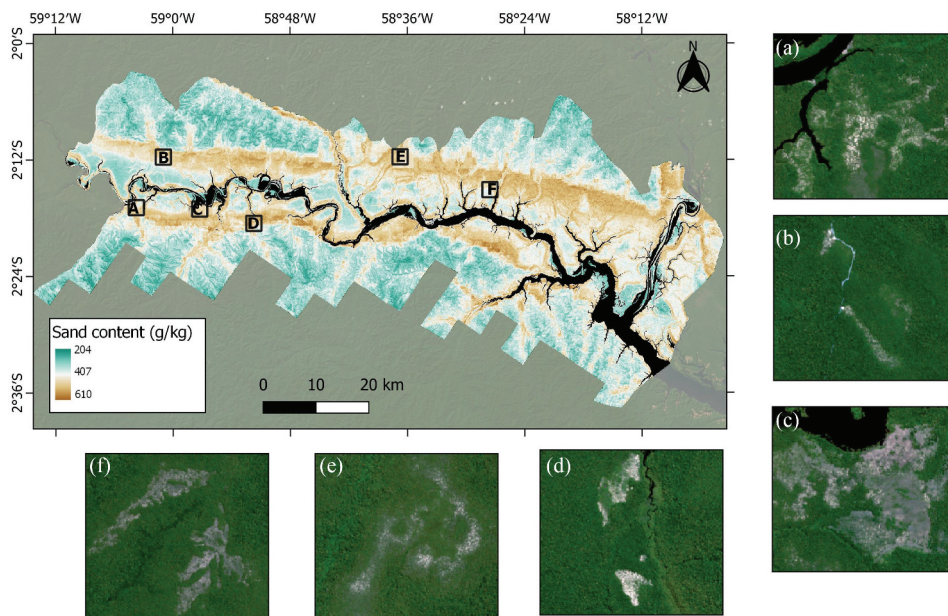


Figure 5. Map of soil sand content in the 100–200 cm layer in the USDR, together with images of open shrubby campinaranas in the RGB composition of the sentinel-2A and Planet/NICFI optical sensors (a, b, c, d, e and f). Orange tones represent a greater amount of sand and green colors a lower sand content.

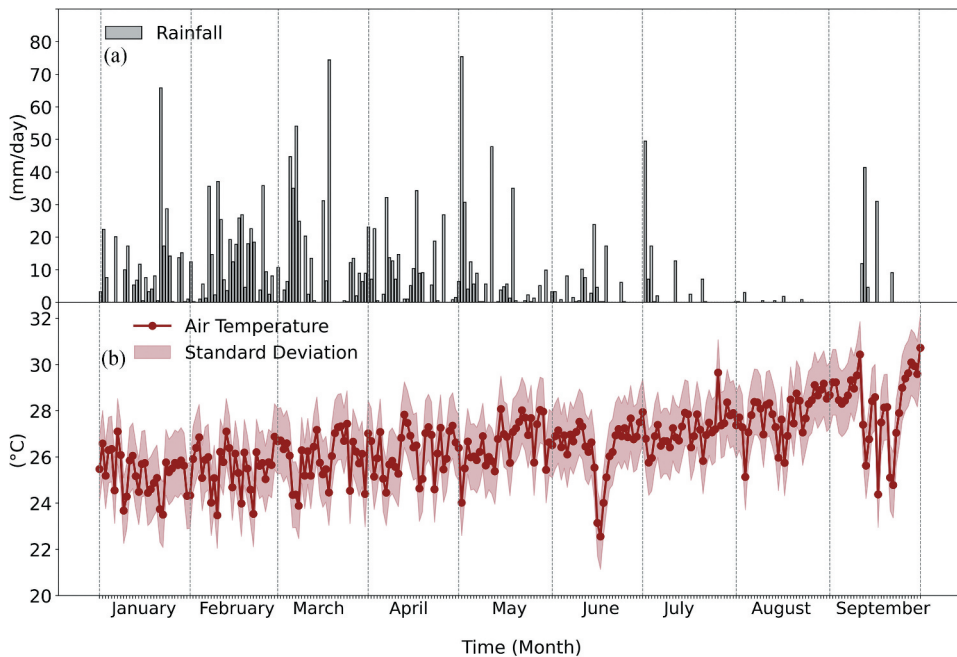


Figure 6. Average daily variability of air temperature and precipitation for January to September 2023 at the ATTO-Campina site.

Figure 6 shows the temporal variability of air temperature and precipitation at the ATTO-Campina site (USDR) between January and September 2023. During the analysed period, the air temperature presented an average daily variability between 24°C and 27°C; however, during some specific days (15 and 16 of June) values close to 22°C were observed due to an incursion of cold air coming from the southern region of Brazil (Camarinha-Neto et al. 2021). In the months with little rain (August and September), the average air temperature in the open shrubby campinarana was close to 30°C.

The hourly variability of air temperature in the open shrubby campinarana was analysed for 2 months of the rainy season and 2 months with less rainfall (Figure 7). The hourly average air temperature was generally the most intense between 9:00 and 19:00 with a value of over 27°C. A more heterogeneous distribution in air temperature values during the afternoon was observed during the rainy months, with a few days exceeding temperatures of 32°C (Figure 7(b)). As the rain begins to decrease (August–September), the air temperature in the open shrubby campinarana increases considerably, presenting up to 39°C in the afternoon (Figure 7(c,d)). These values are similar to the maximum values recorded by Ribeiro and Santos (1975) in an open shrubby campinarana. A similar behaviour was found in a caatinga ecosystem (de Jesus and Santana 2017) and savanna landscapes (Herrero et al. 2019), where the temperatures during the rainy season were milder when compared to the dry season, with higher values in areas with low vegetation. In September, several days with a temperature of 30°C at 21:00 were observed (Figure 7(d)).

The high frequency of elevated temperature values during daytime, together with the lack of rain, makes it possible to extrapolate surface temperature through remote sensing

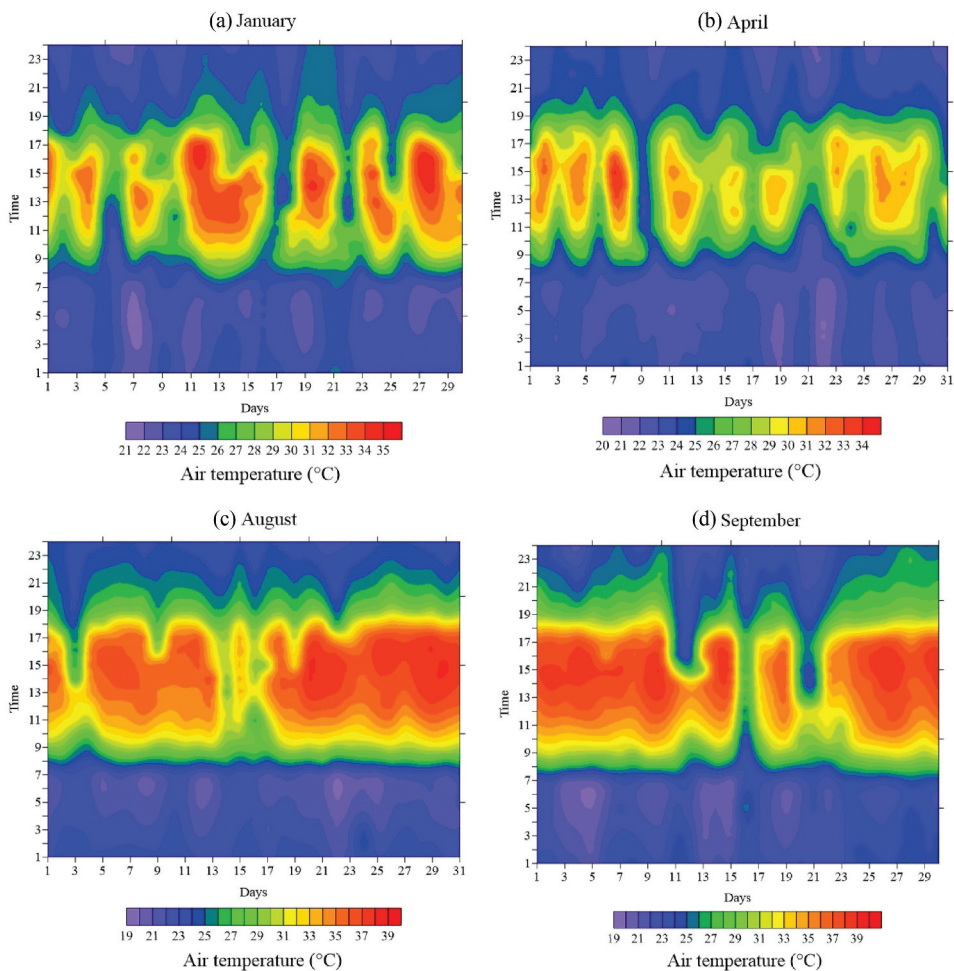


Figure 7. Hourly variability of air temperature in the months of (a) January, (b) April, (c) August and (d) September 2023 at the ATTO-Campina site.

in the dry season of this region. Therefore, the spatial distribution of surface temperature was verified in July 1995 and 2020 in the USDR (Figure 8). The highest surface temperature values performed well, indicating areas of open shrubby campinaranas. Furthermore, very high temperatures were also found in seasonally flooded areas (igapós) along the Uatumã river and its tributaries (Figure 8(a)).

Considering years with little influence from El Niño (1995 and 2020), it was observed that there was a substantial increase in the LST of the campiranas over time (Figure 8). In 1995, the surface temperature during the day ranged from 24°C to 30°C in the open shrubby campinaranas (Figure 8(a)). Twenty-five years later, in 2020, the surface temperature was over 30°C in most open WSEs during the day, with values of up to 40°C being observed in some areas (Figure 8(b)). These results may indicate possible impacts of the ongoing climate change in the Amazon (Marengo et al. 2024; Marengo, Rodrigues-Filho, and Santos 2021). In addition, shrub communities may expand rapidly in response to ongoing climate warming (Wu et al. 2024).

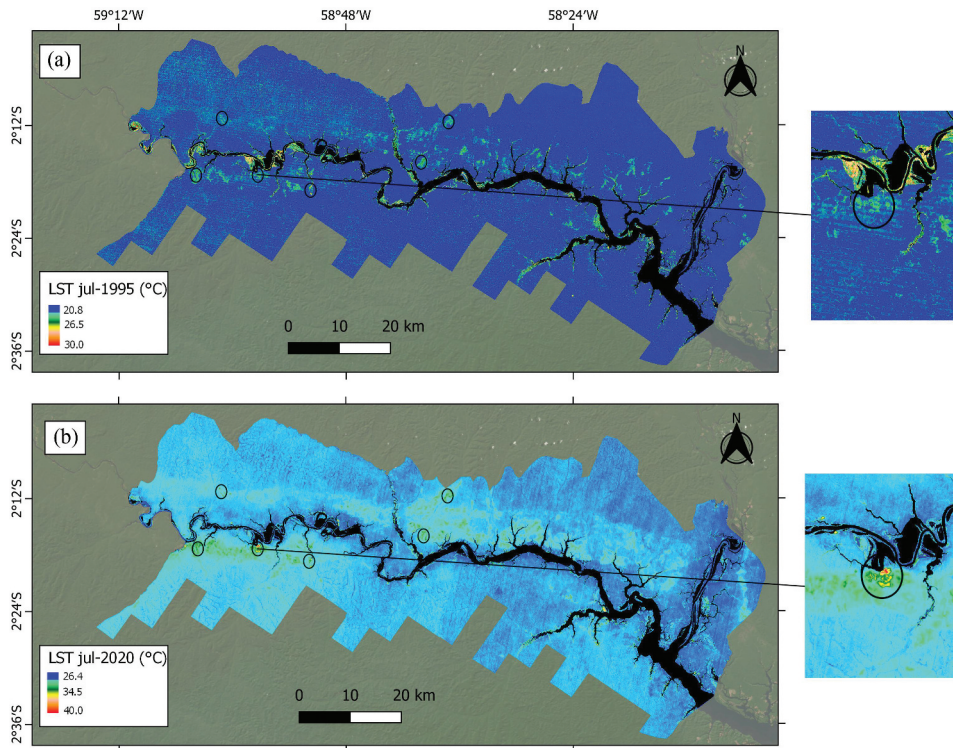


Figure 8. Spatial surface temperature distribution for (a) July 11, 1995 and (b) July 31, 2020 in the USDR. Black circles symbolize open areas of WSEs.

The UAV's thermal infrared camera recorded a maximum surface temperature of 46°C and a minimum of 33°C at the ATTO-Campina site on the morning of 17 September 2022 (Figure 9). The increase in surface temperature makes open WSEs environments more likely to suffer major impacts related to temperature extremes, as recorded during the recent severe droughts (Marengo et al. 2024) and fire events (Adeney, Christensen, and Pimm 2009).

3.3. Classification of WSEs in the USDR

In the next step, we integrated the variables of average surface temperature and canopy height to detect and classify open WSEs areas of the USDR (Figure 10). Open shrubby campinaranas had a canopy height of up to 10 metres (orange tones; Figure 10(a)) and an average surface temperature between 27°C and 32°C (Figure 10(b)). The areas of open shrubby campinaranas observed in the Sentinel 2A and Planet/NICFI satellite images agreed with the values of low canopy height and high average surface temperature. In this way, the mask was determined using the pixel values corresponding to areas with canopy height below 10 metres and surface temperature over 28°C to classify the open shrubby WSEs.

In some areas, the LST values and canopy height of open WSEs showed similarity with other types of surface, as is the case of areas with exposed soil that have suffered some

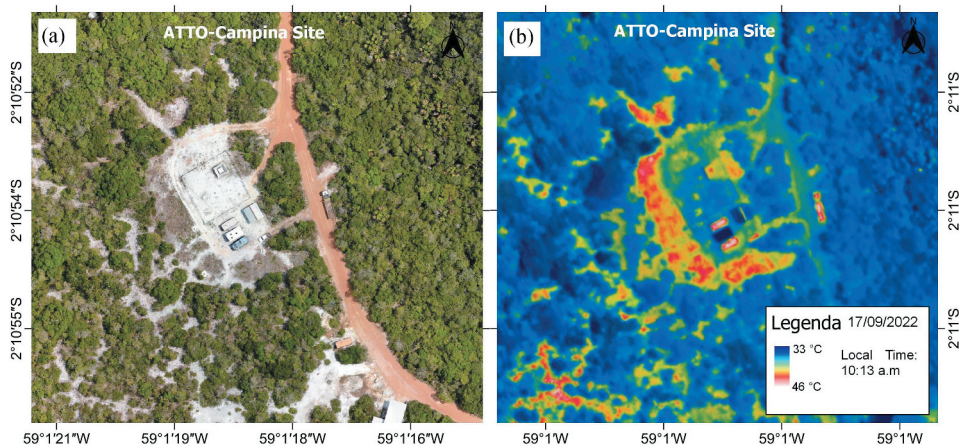


Figure 9. (a) Orthomosaic in the RGB composition of the ATTO-Campina site and (b) land surface temperature of the ATTO-Campina site from UAV images on 09/17/2022 at 10:13 am at a height of 100 m.

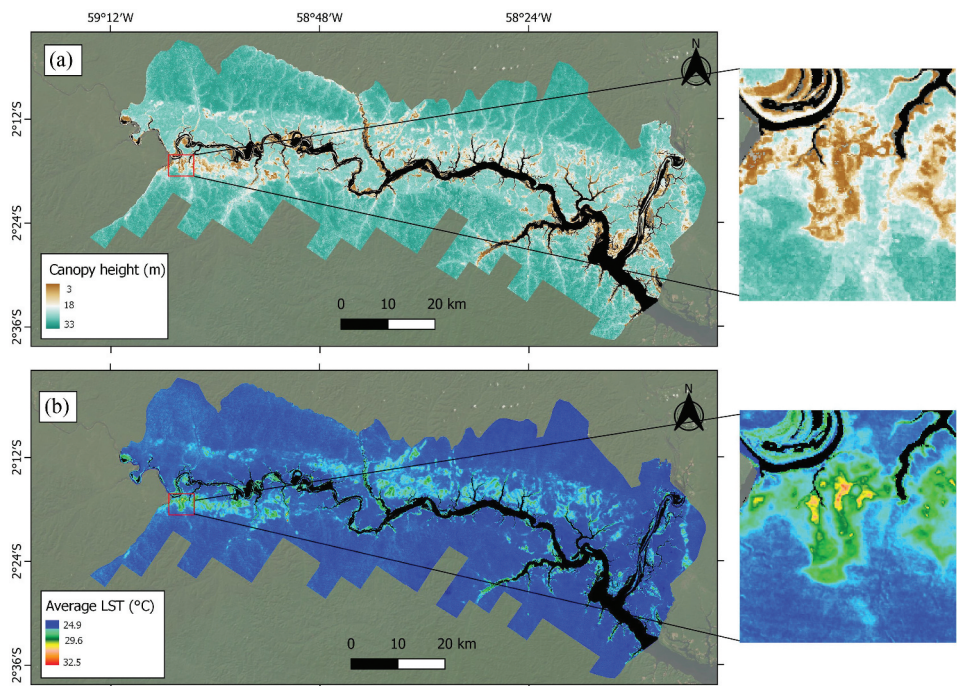


Figure 10. (a) Canopy height in meters and (b) average LST in °C for USDR using GEDI and Landsat data.

type of human intervention (deforested and burnt areas, pastures in the zone of intensive use), and natural areas with low canopy height (igapó and buritizal) that heat a lot during the dry period. To overcome this problem, a filter was applied to the image to eliminate all the pixels that did not correspond to open shrubby areas. To classify all the WSEs (shrub

and forested), a mask was applied, determining a threshold of up to 22 metres in canopy height and an average LST of over 26°C, since forested campinaranas in USDR have taller trees and no areas with exposed sand (Demarchi et al. 2022).

Figure 11 shows the spatial distribution of the WSEs in the USDR. It can be observed that the WSEs are distributed throughout the SCU, with the greatest abundance concentrated north (left bank) of the Uatumã River (Figure 11(a)). Based on the developed method, it was possible to calculate the WSEs coverage with a total area of 31.502 ha, equivalent to around 7.4% of the USDR (424.430 ha). The open shrubby WSEs covered a total area of 3.987 ha, and the forested WSEs 27.515 ha. Many WSEs of the USDR are located where human interference occurred due to extensive and intensive land use (Figure 11(b)). Based on the zoning established for the USDR (IDESAM 2010), areas designated primarily for biodiversity protection harbour 2.426 ha of open WSE formations and 17.883 ha of forested WSE formations. Around 36.6% (1.459 ha) of the open WSEs and 35% (9.632 ha) of the forested WSEs occur within the extensive use zone, while the coverage of the intensive use zone by open WSEs (102 ha) and forested (166 ha) is low. Such information shows that a detailed

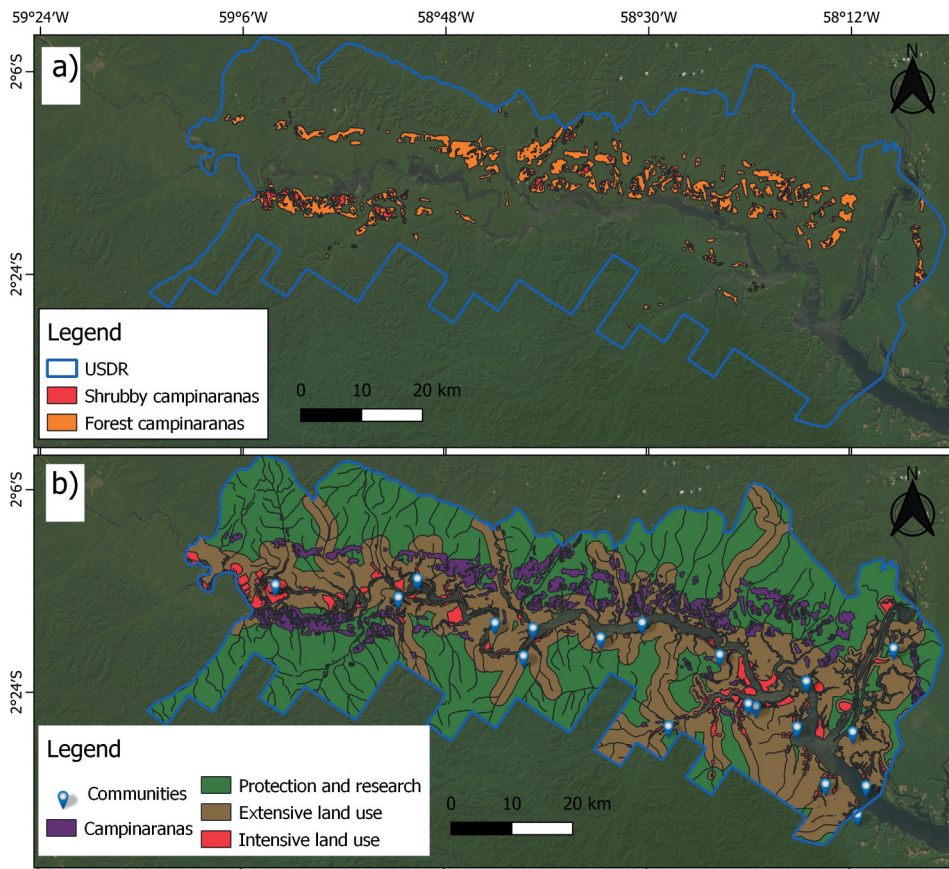


Figure 11. (a) Spatial distribution of WSE macrohabitats in the USDR and (b) occurrence of WSEs in the land use zones established for the USDR.

mapping of the different ecosystems is of great relevance for the reformulation of the SCU management plan since the WSEs are vulnerable ecosystems with low resilience and are not suitable for extensive and intensive use and should, therefore be integrated into the permanent protection zone with some areas destined for the development of guided, community-based ecotourism (Adeney et al. 2016; Demarchi et al. 2024).

4. Conclusions

In this study, we developed a method that allows the detection and classification of WSEs by combining several remote sensors. The analysis of temperature and canopy height is a reliable approach to map WSE environments. Variations in air temperature reflect the extreme microclimatic conditions of this environment. In contrast, the height of the canopy and the surface temperature were essential for distinguishing the types of habitats, with the areas of open shrubby WSEs showing the best performance. Combining these parameters, it was possible to obtain a more accurate and detailed mapping of the WSEs in the USDR, as even small WSE patches could be detected.

WSEs are highly vulnerable to changes in land use such as fires and exploitation of timber and sand resources. For these reasons, WSEs are high priority areas for preserving their biodiversity and associated genetic heritage. In the USDR, the WSEs in the extensive and intensive zones, which represent more than a third of the total coverage of this SCU, should be integrated into the permanent preservation zone to increase its level of protection, allocating specific areas for visits for tourists that are guided by local residents.

The developed method allows further studies in the USDR to understand the environmental dynamics of this ecosystem, for example, to investigate the expansion and retraction of forested formations on open shrubby formations in relation to low-frequency climatic variations and to evaluate the recovery of these environments after anthropogenic disturbances such as fire, as well as to observe trends in temperature increases based on extreme climate indices.

A challenge now is to test the developed method, expanding the mapping and classification of WSEs at basin scales with possible adjustments due to the complexity of these environments. This will allow an accurate estimate of the extent and coverage of these environments in the Amazon, their occurrence at the level of sub-basins and in territories (different types of conservation units, indigenous lands, 'quilombola' lands, undesignated public lands, municipalities, states) and the mapping of disturbances caused by different changes in land use such as fires, mining and palm oil plantations, among others. This has high relevance for public policies in Brazil because, since the ratification of the Ramsar Convention in 1996, the country is committed to defining and classifying its WLs, and evaluating their conditions, implementing government policies aimed at the careful use and conservation of these ecosystems.

Acknowledgments

The authors thank the National Institute for Amazonian Research (INPA), the residents of the Bela Vista and Santa Helena do Abacate communities in the SCU who helped with the fieldwork and the project Amazon Tall Tower Observatory (ATTO) for their support in the development of the research,

as well as the ATTO-Campina Site of the University of São Paulo for the concession of the meteorological data used in this study. This study was supported by the technical/scientific cooperation between INPA and the Max-Planck-Society.

Disclosure statement

No potential conflict of interest was reported by the author(s).

Funding

This research was supported by the Fundação de Amparo à Pesquisa do Estado do Amazonas [FAPEAM] and the Conselho Nacional de Desenvolvimento Científico e Tecnológico [CNPq] via grants from the research projects BIODIVERSA [01.02.016301.03236/2021-74; FAPEAM], PELD [01.02.016301.02630/2022-76; FAPEAM and 441811/2020-5; CNPq], INCT-ADAPTA II [465540/2014-7; CNPq], Fundação Coordenação de Aperfeiçoamento de Pessoal de Nível Superior [CAPES] [PDPG-Amazônia Legal – Process No.[88887.839244/2023-00] and the Geoprocessing and Modeling Laboratory of the Ecology, Monitoring and Sustainable Use of Wetlands [MAUA/INPA] research group. We further acknowledge support of the scientific-technological cooperation between the Max-Planck Society [Germany] and INPA in studies of Amazonian wetlands.

ORCID

Nikolai S. Espinoza  <http://orcid.org/0000-0001-7783-7034>

Rosaria R. Ferreira  <http://orcid.org/0000-0003-0199-5591>

References

- Abraão, M. B., B. W. Nelson, J. C. Baniwa, D. W. Yu, and G. H. Shepard Jr. 2008. "Ethnobotanical Ground-Truthing: Indigenous Knowledge, Floristic Inventories and Satellite Imagery in the Upper Rio Negro, Brazil." *Journal of Biogeography* 35 (12): 2237–2248. <https://doi.org/10.1111/j.1365-2699.2008.01975.x>.
- Adeney, J. M., N. L. Christensen, and S. L. Pimm. 2009. "Reserves Protect Against Deforestation Fires in the Amazon." *PLOS ONE* 4 (4): e5014. <https://doi.org/10.1371/journal.pone.0005014>.
- Adeney, J. M., N. L. Christensen, A. Vicentini, and M. Cohn-Haft. 2016. "White-Sand Ecosystems in Amazonia." *Biotropica* 48 (1): 7–23. <https://doi.org/10.1111/btp.12293>.
- Alnefaie, K. A., and N. H. Abu-Hamdeh. 2020. "Specific Heat and Volumetric Heat Capacity of Some Saudian Soils as Affected by Moisture and Density." *International Journal of Materials Research* 7:42–46. <https://doi.org/10.46300/91018.2020.7.8>.
- Anderson, A. B. 1981. "White-Sand Vegetation of Brazilian Amazonia." *Biotropica* 13 (3): 199–210. <https://doi.org/10.2307/2388125>.
- Andreae, M. O., O. C. Acevedo, A. Araújo, P. Artaxo, C. G. G. Barbosa, H. M. J. Barbosa, J. Brito, et al. 2015. "The Amazon Tall Tower Observatory (ATTO): Overview of Pilot Measurements on Ecosystem Ecology, Meteorology, Trace Gases, and Aerosols." *Atmospheric Chemistry & Physics* 15 (18): 10723–10776. <https://doi.org/10.5194/acp-15-10723-2015>.
- Beck, H. E., N. E. Zimmermann, T. R. McVicar, N. Vergopolan, A. Berg, and E. F. Wood. 2018. "Present and Future Köppen-Geiger Climate Classification Maps at 1-Km Resolution." *Scientific Data* 5 (1): 1–12. <https://doi.org/10.1038/sdata.2018.214>.
- Belloli, T. F., L. A. Guasselli, T. Kuplich, L. F. C. Ruiz, and J. P. D. Simioni. 2022. "Classificação baseada em objeto de tipologias de cobertura vegetal em área úmida integrando imagens ópticas e SAR." *Revista Brasileira de Cartografia* 74 (1): 67–83. <https://doi.org/10.14393/rbvcv74n1-61277>.

- Berhane, T. M., C. R. Lane, Q. Wu, B. C. Autrey, O. A. Anenkhonov, V. V. Chepinoga, and H. Liu. 2018. "Decision Tree, Rule-Based, and Random Forest Classification of High-Resolution Multispectral Imagery for Wetland Mapping and Inventory." *Remote Sensing* 10 (4): 1–26. <https://doi.org/10.3390/rs10040580>.
- Camarinha-Neto, G. F., J. C. Cohen, C. Q. Dias-Júnior, M. Sörgel, J. H. Cattanio, A. Araújo, S. Wolff, P. A. Kuhn, R. A. Souza, and L. V. Rizzo. 2021. "The Friagem Event in the Central Amazon and Its Influence on Micrometeorological Variables and Atmospheric Chemistry." *Atmospheric Chemistry & Physics* 21 (1): 339–356. <https://doi.org/10.5194/acp-21-339-2021>.
- Capurro, J. M. G., S. H. Borges, C. Cornelius, A. Vicentini, E. M. B. Prata, F. M. Costa, P. Campos, A. O. Sawakuchi, F. Rodrigues, A. Zular, et al. 2020. "Patterns and Processes of Diversification in Amazonian White Sand Ecosystems: Insights from Birds and Plants." In *Neotropical Diversification: Patterns and Processes. Fascinating Life Sciences*, edited by V. Rull and A. Carnaval. Cham: Springer. https://doi.org/10.1007/978-3-030-31167-4_11.
- Carneiro, A., and R. Trancoso. 2007. *Levantamento do meio físico da Reserva de Desenvolvimento Sustentável da RDS do Uatumã*. Manaus, Brazil: Instituto de Conservação e Desenvolvimento Sustentável do Amazonas.
- Carvalho, T. C., F. Wittmann, M. T. F. Piedade, A. F. Resende, T. S. F. Silva, and J. Schöngart. 2021. "Fires in Amazonia Blackwater Floodplain Forests: Causes, Human Dimension and Implications for Conservation." *Frontiers in Forests and Global Change* 4:755441. <https://doi.org/10.3389/ffgc.2021.755441>.
- Cordeiro, C. L. O., and D. F. Rossetti. 2015. "Mapping Vegetation in a Late Quaternary Landform of the Amazonian Wetlands Using Object-Based Image Analysis and Decision Tree Classification." *International Journal of Remote Sensing* 36 (13): 3397–3422. <https://doi.org/10.1080/01431161.2015.1060644>.
- Damasco, F. M., A. Vicentini, C. V. Castilho, T. P. Pimentel, and H. E. M. Nascimento. 2013. "Disentangling the Role of Edaphic Variability, Flooding Regime and Topography of Amazonian White-Sand Vegetation." *Journal of Vegetation Science* 24 (2): 384–394. <https://doi.org/10.1111/j.1654-1103.2012.01464.x>.
- de Almeida, D. R. A., L. B. Vedovato, M. Fuza, P. Molin, H. Cassol, A. F. Resende, P. M. Krainovic, et al. 2025. "Remote Sensing Approaches to Monitor Tropical Forest Restoration: Current Methods and Future Possibilities." *The Journal of Applied Ecology* 62 (2): 188–206. <https://doi.org/10.1111/1365-2664.14830>.
- de Jesus, J. B., and I. D. M. Santana. 2017. "Estimation of Land Surface Temperature in Caatinga Area Using Landsat 8 Data." *Journal of Hyperspectral Remote Sensing* 7 (3): 150–157. <https://doi.org/10.29150/jhrs.v7.3.p150-157>.
- Demarchi, L. O., V. P. Klein, D. P. P. Aguiar, L. C. Marinho, M. J. Ferreira, A. Lopes, J. Cruz, et al. 2022. "The Specialized White-Sand Flora of the Uatumã Sustainable Development Reserve, Central Amazon, Brazil." *Check List* 18 (1): 187–217. <https://doi.org/10.15560/18.1.187>.
- Demarchi, L. O., V. P. Klein, J. Schöngart, F. Wittmann, and M. T. F. Piedade. 2024. "As formações vegetais amazônicas sobre areias brancas: campinaranas." In *Inventário das áreas úmidas brasileiras: Distribuição, ecologia, manejo, ameaças e lacunas de conhecimento*, edited by W. J. Junk and C. Nunes da Cunha, 720. Cuiabá, Brazil: Carlini & Caniato Editorial.
- Dronova, I. 2015. "Object-Based Image Analysis in Wetland Research: A Review." *Remote Sensing* 7 (5): 6380–6413. <https://doi.org/10.3390/rs70506380>.
- Fassoni-Andrade, A. C., A. S. Fleischmann, F. Papa, R. C. D. D. Paiva, S. Wongchuig, J. M. Melack, A. A. Moreira, et al. 2021. "Amazon Hydrology from Space: Scientific Advances and Future Challenges." *Reviews of Geophysics* 59 (4): 1–97. <https://doi.org/10.1029/2020RG000728>.
- Ferreira-Ferreira, J., T. S. F. Silva, A. S. Streher, A. G. Affonso, L. F. A. Furtado, B. R. Forsberg, J. Valsecchi, H. L. Queiroz, and E. M. L. M. Novo. 2015. "Combining ALOS/PALSAR Derived Vegetation Structure and Inundation Patterns to Characterize Major Vegetation Types in the Mamirauá Sustainable Development Reserve, Central Amazon Floodplain, Brazil." *Wetlands Ecology and Management* 23 (1): 41–59. <https://doi.org/10.1007/s11273-014-9359-1>.

- Fleischmann, A. S., F. Papa, J. M. Melack, A. Fassoni-Andrade, S. Wongchuig, R. C. D. Paiva, S. K. Hamilton, et al. 2022. "How Much Inundation Occurs in the Amazon River Basin?" *Remote Sensing Environment* 278:113009. <https://doi.org/10.1016/j.rse.2022.113099>.
- Franco, W., and N. Dezzio. 1994. "Soils and Soil-Water Regime in the Terra-Firme-Caatinga Forest Complex Near San Carlos de Rio Negro, State of Amazonas, Venezuela." *Interciencia* 19:305–316.
- Herrero, H. V., J. Southworth, E. Bunting, R. R. Kohlhaas, and B. Child. 2019. "Integrating Surface-Based Temperature and Vegetation Abundance Estimates into Land Cover Classifications for Conservation Efforts in Savanna Landscapes." *Sensors (Switzerland)* 19 (16): 3456. <https://doi.org/10.3390/s19163456>.
- Householder, J. E., F. Wittmann, J. Schöngart, M. T. F. Piedade, W. J. Junk, E. M. Latrubesse, A. C. Quaresma, et al. 2024. "One Sixth of Amazonian Tree Diversity is Dependent on River Floodplains." *Nature Ecology & Evolution* 8 (5): 901–911. <https://doi.org/10.1038/s41559-024-02364-1>.
- IBGE. 2012. *Manual técnico da vegetação brasileira*. 2nd ed. Rio de Janeiro, Brazil: Instituto Brasileiro de Geografia e Estatística.
- IDESAM. 2009. *Série técnica planos de gestão: Reserva de Desenvolvimento Sustentável do Uatumã*. Manaus, Brazil: Instituto de Conservação e Desenvolvimento Sustentável do Amazonas.
- IDESAM. 2010. *Plano de uso público: Ordenamento turístico da Reserva de Desenvolvimento Sustentável do Uatumã*. Manaus, Brazil: Instituto de Conservação e Desenvolvimento Sustentável do Amazonas.
- Junk, W. J., and C. N. Cunha. 2024. *"Inventário das áreas úmidas brasileiras: distribuição, ecologia, manejo, ameaças e lacunas de conhecimento"*. 1st ed. [recurso digital]. Cuiabá, Brazil: Carlini & Caniato Editorial.
- Junk, W. J., M. T. F. Piedade, M. Cohn-Haft, J. M. Adeney, F. Wittmann, and F. Wittmann. 2011. "A Classification of Major Naturally-Occurring Amazonia Lowland Wetlands." *Wetlands* 31 (4): 623–640. <https://doi.org/10.1007/s13157-011-0190-7>.
- Junk, W. J., M. T. F. Piedade, R. Lourival, F. Wittmann, P. Kandus, L. D. Lacerda, R. L. Bozelli, et al. 2014. "Brazilian Wetlands: Their Definition, Delineation, and Classification for Research, Sustainable Management, and Protection." *Aquatic Conservation: Marine and Freshwater Ecosystems* 24 (1): 5–22. <https://doi.org/10.1002/aqc.2386>.
- Junk, W. J., M. T. F. Piedade, J. Schöngart, and F. Wittmann. 2012. "A Classification of Major Natural Habitats of Amazonian White-Water River Floodplains (Várzeas)." *Wetlands Ecology and Management* 20 (6): 461–475. <https://doi.org/10.1007/s11273-012-9268-0>.
- Kubitzki, K. 1989. "Amazon Lowland and Guayana Highland – Historical and Ecological Aspects of the Development of Their Floras." *Amazoniana* 11:1–12.
- Lobo, G. S., F. Wittmann, and M. T. F. Piedade. 2019. "Response of Black-Water Floodplain (Igapó) Forests to Flood Pulse Regulation in a Dammed Amazonian River." *Forest Ecology & Management* 434:110–118. <https://doi.org/10.1016/j.foreco.2018.12.001>.
- Mahdianpari, M., B. Salehi, F. Mohammadimanesh, S. Homayouni, and E. Gill. 2019. "The First Wetland Inventory Map of Newfoundland at a Spatial Resolution of 10 M Using Sentinel-1 and Sentinel-2 Data on the Google Earth Engine Cloud Computing Platform." *Remote Sensing* 11 (1): 43. <https://doi.org/10.3390/rs11010043>.
- Maltchik, L., V. Caleffi, C. Stenert, D. Batzer, M. T. F. Piedade, and W. J. Junk. 2017. "Legislation for Wetland Conservation in Brazil: Are Existing Terms and Definitions Sufficient?" *Environmental Conservation* 45 (3): 301–305. <https://doi.org/10.1017/S0376892917000522>.
- Marengo, J. A., J. C. Espinoza, R. Fu, J. C. Jimenez Muñoz, L. M. Alves, H. R. da Rocha, and J. Schöngart. 2024. "Long-Term Variability, Extremes and Changes in Temperature and Hydrometeorology in the Amazon Region: A Review." *Acta Amazonica* 54 (spe1): e54es22098. <https://doi.org/10.1590/1809-4392202200980>.
- Marengo, J. A., S. Rodrigues-Filho, and D. V. Santos. 2021. "Impacts, Vulnerability and Adaptation to Climate Change in Brazil: An Integrated Approach." *Sustainability in Debate* 11 (3): 14–23. <https://doi.org/10.18472/SustDeb.v11n3.2020.35624>.

- Mendonça, B. A. F., E. I. F. Filho, C. E. G. R. Schaefer, F. N. B. Simas, and M. D. de Paula. 2015. "OS SOLOS DAS CAMPINARANAS NA AMAZÔNIA BRASILEIRA: ECOSSISTEMAS ARENÍCOLAS OLIGOTRÓFICOS." *Ciência Florestal* 25 (4): 827–839. <https://doi.org/10.5902/1980509820581>.
- Ndossi, M. I., and U. Avdan. 2016. "Application of Open-Source Coding Technologies in the Production of Land Surface Temperature (LST) Maps from Landsat: A Pyqgis Plugin." *Remote Sensing* 8 (5): 413. <https://doi.org/10.3390/rs8050413>.
- Piedade, M. T. F., P. Parolin, A. Lopes, F. Wittmann, W. J. Junk, A. Mortati, T. André, and J. Schöngart. 2025. "Amazonian Rivers from the Guiana Shield." In *Rivers of South America*, edited by M. A. S. Graça, M. Callisto, F. T. de Mello, and D. Rodríguez-Olarte, 239–277. Elsevier. <https://doi.org/10.1016/B978-0-12-823429-7.00003-3>.
- Potapov, P., X. Li, A. Hernandez-Serna, A. Tyukavina, M. C. Hansen, A. Kommareddy, A. Pickens, et al. 2021. "Mapping Global Forest Canopy Height Through Integration of GEDI and Landsat Data." *Remote Sensing Environment* 253:112165. <https://doi.org/10.1016/j.rse.2020.112165>.
- Prance, G. T. 1996. "Islands in Amazonia." *Philosophical Transactions of the Royal Society* 351:823–833.
- Quesada, C. A., J. Lloyd, L. O. Anderson, N. M. Fyllas, M. Schwarz, and C. I. Czimczik. 2011. "Soils of Amazonia with Particular Reference to the RAINFOR Sites." *Biogeosciences* 8 (6): 1415–1440. <https://doi.org/10.5194/bg-8-1415-2011>.
- Rennó, C. D., A. D. Nobre, L. A. Cuartas, and J. V. Soares. 2008. "HAND, a New Terrain Descriptor Using SRTM-DEM: Mapping Terra-Firme Rainforest Environments in Amazonia." *Remote Sensing Environment* 112 (9): 3469–3481. <https://doi.org/10.1016/j.rse.2008.03.018>.
- Resende, A. F., J. Schöngart, A. S. Streher, J. Ferreira-Ferreira, M. T. F. Piedade, and T. S. F. Silva. 2019. "Massive Tree Mortality from Flood-Pulse Disturbances in Amazonian Floodplain Forests: The Collateral Effects of Hydropower Production." *Science of the Total Environment* 659:587–598. <https://doi.org/10.1016/j.scitotenv.2018.12.208>.
- Ribeiro, M. N. G., and A. Santos. 1975. "Observações microclimáticas no ecossistema Campina Amazônica." *Acta Amazonica* 5 (2): 183–189. <https://doi.org/10.1590/1809-43921975052183>.
- Rosetti, D. F., G. M. Moulatlet, H. Tuomisto, R. Gribel, P. M. Toledo, M. M. Valeriano, K. Ruokolainen, et al. 2019. "White Sand Vegetation in an Amazonian Lowland Under the Perspective of a Young Geological History." *Anais da Academia Brasileira de Ciências* 91 (4): 4. <https://doi.org/10.1590/0001-3765201920181337>.
- Schöngart, J., F. Wittmann, A. F. Resende, C. Assahira, G. S. Lobo, J. R. D. Neves, M. da Rocha, et al. 2021. "The Shadow of the Balbina Dam: A Synthesis of Over 35 Years of Downstream Impacts on Floodplain Forests in Central Amazonia." *Aquatic Conservation: Marine and Freshwater Ecosystems* 31 (5): 1117–1135. <https://doi.org/10.1002/aqc.3526>.
- Targhetta, N., J. Kesselmeier, and F. Wittmann. 2015. "Effects of the Hydroedaphic Gradient on Tree Species Composition and Aboveground Wood Biomass of Oligotrophic Forest Ecosystems in the Central Amazon Basin." *Folia Geobotanica* 50 (3): 185–205. <https://doi.org/10.1007/s12224-015-9225-9>.
- Tian, S., X. Zhang, J. Tian, and Q. R. Sun. 2016. "Random Forest Classification of Wetland Land Covers from Multisensory Data in the Arid Region of Xinjiang, China." *Remote Sensing* 8 (11): 954. <https://doi.org/10.3390/rs8110954>.
- Vasques, G. M., M. R. Coelho, R. O. Dart, L. C. Cintra, and J. F. M. Baca. 2021. "Soil Clay, Silt and Sand Content Maps for Brazil at 0-5, 5-15, 15-30, 30-60, 60-100 and 100-200 Cm Depth Intervals with 90 M Spatial Resolution." *Embrapa Solos, Empresa Brasileira de Pesquisa Agropecuária, Brasília, Brazil* (5).
- Veloso, H. P., A. L. R. Rangel Filho, and J. C. A. Lima. 1991. *Classificação da vegetação brasileira, adaptada a um sistema universal*. Rio de Janeiro, Brazil: Instituto Brasileiro de Geografia e Estatística.
- Wang, X., X. Gao, Y. Zhang, X. Fei, Z. Chen, J. Wang, Y. Zhang, X. Lu, and H. Zhao. 2019. "Land-Cover Classification of Coastal Wetlands Using the RF Algorithm for Worldview-2 and Landsat 8 Images." *Remote Sensing* 11 (16): 1927. <https://doi.org/10.3390/rs11161927>.
- Wu, Z., W. Wang, W. Zhu, P. Zhang, R. Chang, and G. Wang. 2024. "Shrub Ecosystem Structure in Response to Anthropogenic Climate Change: A Global Synthesis." *Science of the Total Environment* 953:176202. <https://doi.org/10.1016/j.scitotenv.2024.176202>.